Biolabeling

DOI: 10.1002/anie.201007215

Superresolution Imaging of Albumin-Conjugated Fluorescent Nanodiamonds in Cells by Stimulated Emission Depletion**

*Yan-Kai Tzeng, Orestis Faklaris, Be-Ming Chang, Yung Kuo, Jui-Hung Hsu, and Huan-Cheng Chang**

Since the discovery of fullerenes and carbon nanotubes, carbon-based nanomaterials have been considered the key materials of the 21st century.[1] In comparison with other nanoscale carbon allotropes, nanodiamond is unique in that it consists solely of sp^3-hybridized carbon atoms and thus is optically transparent and biologically inert. The material often contains point defects, such as nitrogen-vacancy complexes (e.g. NV^-), which form photoluminescent color centers.[2] These built-in fluorophores are atomlike and exceptionally photostable. No sign of photobleaching was detected even under continuous high-power laser excitation at the single-molecule level.[3] The combination of these features has made fluorescent nanodiamond (FND),[4] which contains a high concentration of NV^- centers, an appealing alternative to organic dyes, fluorescent proteins, and potentially toxic quantum dots as a biolabel for long-term in vitro and in vivo imaging applications.[5–10]

Although FNDs hold great potential for use in biology and medicine,[11,12] little is known about how they behave in biological systems with nanoscale precision and resolution. With the advent of superresolution far-field fluorescence microscopy,[13] it is now possible to obtain diffraction-unlimited images of FNDs. By using stimulated emission depletion (STED) microscopy, Hell, Eggeling, and co-workers demonstrated a remarkably high resolution of approximately 6 nm for single NV^- centers in bulk diamond[14] and achieved an up to sixfold improvement in resolution over confocal fluorescence microscopy for 35 nm FNDs dispersed on a glass slide.[15] Such an improvement is crucial for revealing the detailed structures of biological macromolecular complexes and assemblies, including cellular organelles and subcellular compartments. We aimed to extend these superresolution studies on FNDs to cellular-imaging applications.

For the use of FND as a fluorescent label or marker for superresolution imaging in cells, particle agglomeration is the first hurdle to overcome. Like many other nanoparticles, FNDs (or NDs in general) are prone to precipitation in a physiological environment.[16,17] This characteristic makes homogeneous cell labeling and/or labeling of non-adherent cells (or suspension cells) with these fluorescent particles very difficult, if not impossible. Lim et al.[18] recently studied systematically the stabilization of nanoparticles (specifically, iron oxide core/gold shell nanoparticles) in media with a high ionic strength, such as phosphate-buffered saline (PBS), a common biological buffer. They found that bovine serum albumin (BSA) was a better stabilizing agent than polyethylene glycol, and that the BSA-coated nanoparticles could resist flocculation for more than 5 days in PBS. Such a colloid-stabilization effect has similarly been observed for quantum dots[19] and nanogold particles.[20] In this study, we coated 30 nm FNDs *noncovalently* with BSA to prevent FND agglomeration in PBS and cell medium. Additionally, we found that α-lactalbumin (α-LA),[21] which has an isoelectric point (pI = 4–5) close to that of BSA but is approximately four times smaller in terms of mass, can serve the same purpose.

We produced carboxylated/oxidized FNDs with a size in the range of 30 nm by helium-ion irradiation and thermal annealing of type Ib diamond nanocrystallites, followed by oxygen etching in air and surface functionalization of the particles in strong oxidative acids.[22] FNDs were coated with BSA (or α-LA) by physical adsorption through vortex mixing of the acid-treated FNDs with the proteins in acidic water (pH 4.5). According to the experimental procedures detailed in references [14] and [15], a STED microscope was built in-house to acquire superresolution images of FNDs on glass substrates and in cells, in particular, HeLa cells (see Figure S1 in the Supporting Information for experimental details). With both the excitation laser ($\lambda_{ex} = 532$ nm) and the depletion laser ($\lambda_{ex} = 740$ nm) operating in continuous-wave (CW) mode, a lateral resolution in the range of 40 nm was readily achieved (see Figure S2). To label cells with FNDs, we employed two different approaches to deliver the nanoparticles into the cell cytoplasm: electroporation and endocytosis. In the first approach, an externally applied electric field is used to increase the permeability of the cell plasma

[*] Y.-K. Tzeng,[+] Dr. O. Faklaris,[+] Dr. H.-C. Chang
Institute of Atomic and Molecular Sciences
Academia Sinica, Taipei, 106 (Taiwan)
Fax: (+886) 2-2362-0200
E-mail: hcchang@po.iams.sinica.edu.tw
Y.-K. Tzeng,[+] Y. Kuo, Dr. H.-C. Chang
Department of Chemistry, National Taiwan University
Taipei, 106 (Taiwan)
B.-M. Chang, Dr. H.-C. Chang
Department of Chemistry, National Taiwan Normal University
Taipei, 106 (Taiwan)
Dr. J.-H. Hsu
Department of Materials Science and Optoelectronic Science
National Sun Yat-Sen University, Kaohsiung 804 (Taiwan)
[+] These authors contributed equally.

[**] This research was supported by the Academia Sinica and the National Science Council, Taiwan with Grant No. 99-2119M-001-026-. We thank Dr. K. Y. Han and Dr. C. Eggeling at the Max Planck Institute for Biophysical Chemistry in Göttingen (Germany) for instruction and assistance in setting up the STED system.

Supporting information for this article is available on the WWW under http://dx.doi.org/10.1002/anie.201007215.

membrane, which leads to accumulation of the particles in the cell.[23] The second method is based on the ability of cells to endocytose: a process by which cells take up particles either physically bound to or located in the vicinity of the plasma membrane.[24] With STED microscopy, we were able to identify individual FND particles in cells and distinguish them from particle aggregates trapped in endosomes.

Our previous experiments demonstrated that the acid-washed diamond nanoparticles have an exceptionally high affinity for various types of proteins in PBS.[25] This high affinity is established as a result of the interplay of electrostatic forces, hydrogen bonding, and hydrophobic interactions between the adsorbent and the adsorbate. The loading capacity is maximized at pH values close to the pI values of the individual proteins investigated. For the 30 nm FNDs used in this study, a weight ratio of BSA/FND $\approx$ 1:1 (or α-LA/FND $\approx$ 3:1) was chosen to ensure complete saturation of the particle surface with the protein molecules (see Figure S3 for titration experiments).[25] Figure 1a shows typical size distributions of 30 nm FNDs before and after noncovalent conjugation with BSA and α-LA in distilled deionized water (DDW) or PBS, as determined by dynamic light scattering. Although low agglomeration was observed for bare FND in DDW, its size drastically increased by a factor of more than 20 in PBS. With the albumin coating, the particle-agglomeration effect was greatly suppressed. The mean size of the particles increased only from 30 to 42 nm after conjugation with BSA and from 30 to 35 nm after conjugation with α-LA. Such size differences indicate monolayer coverages of both proteins on the particle surfaces. In analogy with our previous findings for cytochrome *c* on NDs,[26] both noncovalently bound nanoparticle bioconjugates were highly stable in PBS, and their sizes were essentially unchanged after five cycles of washing to remove unbound proteins in solution. Moreover, the good stability was preserved even when the nanoparticle bioconjugates were dispersed in PBS at a concentration as high as 1 mg mL^{-1} for 9 days (Figure 1b).

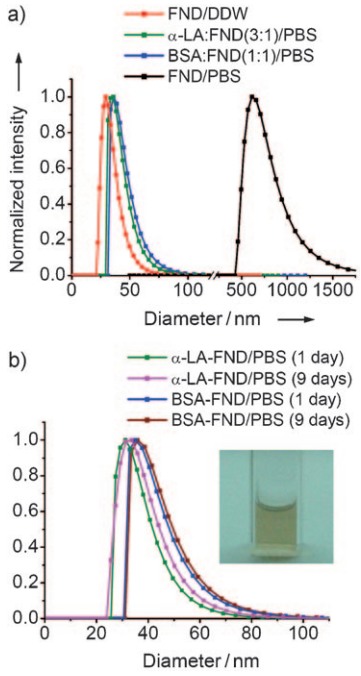

Figure 1. Size measurement of FNDs by dynamic light scattering. a) Size distributions of FNDs before and after noncovalent conjugation with BSA and α-LA in DDW and PBS. The mean diameters of the particles with size distributions from left to right are 30.0, 35.1, 41.9, and 752.7 nm. b) Stability tests of the colloidal suspensions of BSA-conjugated FNDs and α-LA-conjugated FNDs in PBS at room temperature for 9 days. The mean diameters of the particles with size distributions from left to right are 35.0, 37.0, 41.9, and 43.2 nm. Inset: Photograph showing the good dispersibility of BSA-conjugated FNDs in PBS (1 mg mL^{-1}) after 1 day.

The first method we applied to deliver the colloidally stable FNDs into cells was electroporation. Figure 2a shows a confocal fluorescence image of a HeLa cell recovered from electroporation in a suspension of BSA-conjugated FNDs and grown at 37 °C. Three-dimensional scans of the specimen confirmed internalization of the FND particles in the cell (see Figure S4). Like typical confocal microscopy, the imaging yielded a diffraction-limited resolution of approximately 230 nm (Figure 2b), which is about six times larger than the mean size of the particles. This resolution is clearly not sufficient to reveal whether the internalized FND particles are fully dispersed or agglomerated in the cytoplasm. STED microscopy, in contrast, can achieve a resolution of about 40 nm (see Figure S5 for the depletion curve), which enables identification of the internalized particles individually (Figure 2c). From a systematic inspection of more than 15 particles in five different cells, we found only occasionally clusters composed of a maximum of two FND particles. This result verifies that electroporation is a technique capable of delivering nanoparticles one by one into living cells through transient pores created in the plasma membrane.

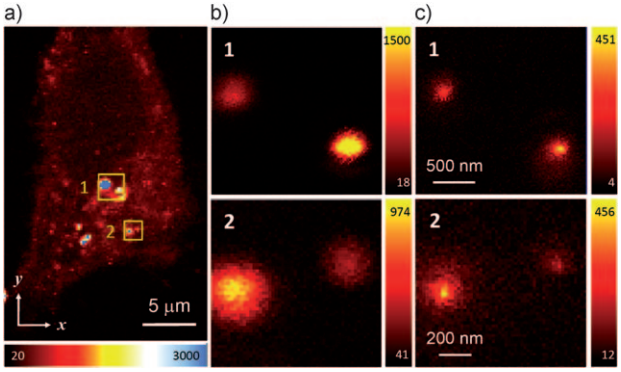

Figure 2. Confocal and STED imaging of HeLa cells labeled with BSA-conjugated FNDs by electroporation. a) Confocal image acquired by raster scanning of an FND-labeled cell. b) Confocal and c) STED images of single BSA-conjugated FND particles enclosed within the yellow boxes "1" and "2" in (a).

Despite this success, a disadvantage of the electroporation method is that the amount of the particles delivered into the cells is low. Moreover, only about 40% of the cells survive the electroporation process. To circumvent this problem, we let BSA-conjugated FNDs be internalized passively by cells

through endocytosis. In this experiment, we first labeled HeLa cells nonspecifically with BSA-conjugated FNDs by physical adsorption at 4 °C, where endocytosis is inhibited,[27,28] and then recultured them in culture medium at 37 °C to facilitate internalization of the FNDs bound to the cell membrane. The acquired confocal images (Figure 3a) show clearly that more FNDs were internalized in the cytoplasm than by electroporation, although a threefold lower concentration of FNDs was used for labeling. Furthermore, the majority (> 90 %) of the FNDs observed were in an isolated form, as evidenced by STED imaging with a subdiffraction resolution of approximately 40 nm (Figure 3b,c). This observation stands in interesting contrast to the case when the same cells were labeled with bare FNDs by endocytosis (Figure 4a).[5,8,28–30] In the absence of the BSA coating, the fluorescence intensities as well as the spatial distribution of the internalized FND particles in the cells were highly heterogeneous, and many large agglomerates (only about 50 % of the observed fluorescence spots were diffraction-limited) were found in the cytoplasms (Figure 4b,c; see Figure S6 for further details).

To summarize, we have illustrated the potential use of albumin-conjugated FNDs for homogeneous labeling and their superresolution imaging in cells by STED microscopy. The conjugation method is simple and straightforward, and does not involve a covalent cross-linkage. Of particular importance is the coating of FNDs with α-LA, which offers the advantages that it produces smaller particles and imposes fewer constraints on the functionality of bioactive molecules for subsequent conjugation. We have prepared colloidally stable α-LA-coated FNDs as small as 18 nm (see Figure S7 in the Supporting Information).[31] These tiny particles are promising biolabels having a size comparable to that of bioconjugated quantum dots. Since albumins are amenable to coupling with biotin,[32] the albumin-modified FND particles can be readily conjugated with avidin (or streptavidin) and subsequently with biotinylated antibodies for high-specificity targeting and imaging applications. In light of the fact that fluorescent nanoparticles are viewed as an innovative technology for future biomedical applications, we anticipate that this emerging type of carbon-based nanoparticles will find increasing use as photostable biolabels as well as long-term cell trackers. The combination of the perfect photostability of FND with the subdiffraction-imaging capability of STED microscopy is expected to open up many exciting new opportunities to probe intracellular interactions and dynamics, not only with single-particle sensitivity but also with nanometric resolution and precision.

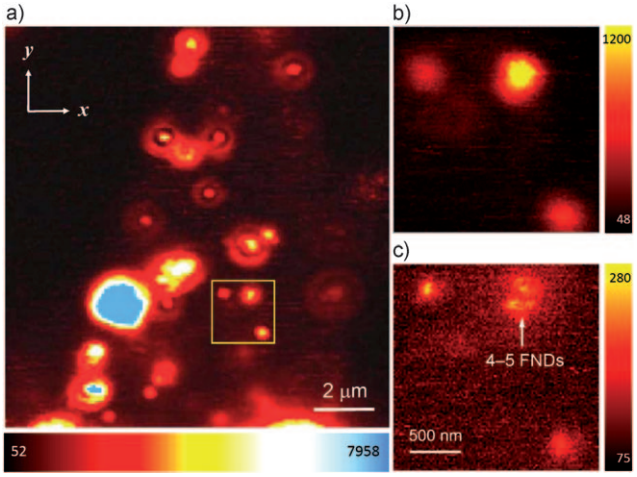

Figure 4. Confocal and STED imaging of HeLa cells labeled with bare FNDs by endocytosis. a) Confocal image acquired by raster scanning of an FND-labeled cell. b) Confocal and c) STED images of bare FND particles enclosed within the yellow box in (a). The cluster indicated by the white arrow in (c) is composed of up to five FND particles.

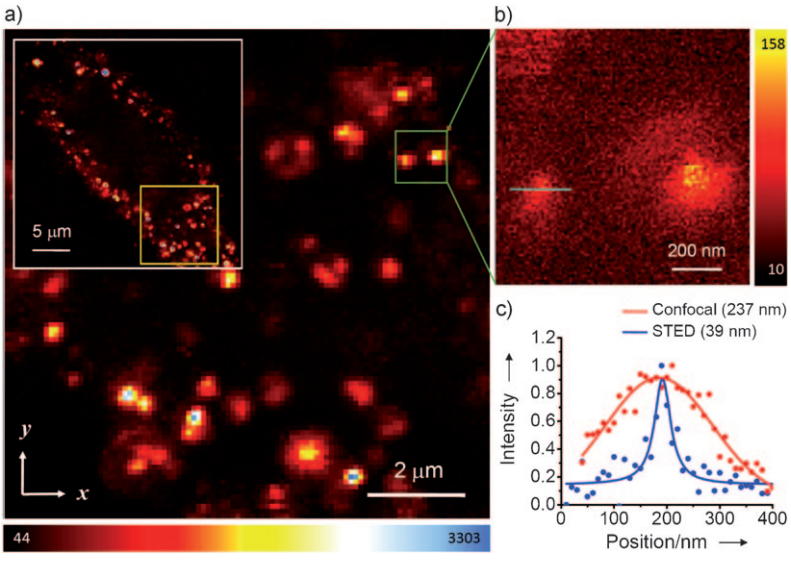

Figure 3. Confocal and STED imaging of HeLa cells labeled with BSA-conjugated FNDs by endocytosis. a) Confocal image acquired by raster scanning of an FND-labeled cell. The fluorescence image of the entire cell is shown in the white box and demonstrates fairly uniform cell labeling by BSA-conjugated FNDs. b) STED image of single BSA-conjugated FND particles enclosed within the green box in (a). c) Confocal and STED fluorescence intensity profiles of the particle indicated in (b) with a blue line. Solid curves are best fits to one-dimensional Gaussian (confocal) or Lorentzian (STED) functions. The corresponding full widths at half-maximum are given in parentheses.

Experimental Section

Procedures for the production of FNDs have been described in detail in Refs. [22,29] and can be found in the Supporting Information. For bioconjugation by physical adsorption, acid-washed FNDs (1 mg) were first thoroughly sonicated in DDW for 30 min and then mixed with BSA (1 mg) or α-LA (3 mg) in acidic water (pH value adjusted to 4.5 with HCl) by gentle vortex mixing for 1 h. Unbound protein molecules were removed by washing the nanoparticle bioconjugates once in DDW and five times in PBS by using centrifugal filter devices (Amicon Ultra-15, 100 K or Amicon Ultra-4, 3 K, Millipore). Size distributions of the FND particles before and after bioconjugation were determined by using a particle-size and zeta-potential analyzer (Delsa Nano C, Beckman-Coulter).

For biolabeling by electroporation, about 10^7 Hela cells were trypsinized, collected, and resus-

pended in serum-free Dulbecco modified Eagle medium (DMEM) containing BSA-conjugated FNDs (500 μg mL^{-1}). The FND–cell solution was then pipetted into a 4 mm electroporation cuvette and incubated in ice for 10 min. Four consecutive 20 ms pulses (with a voltage of 375 V per pulse) were applied to the mixed solution by using an electroporator (Gene Pulser Xcell, Bio-Red). Immediately after electroporation, cells were cooled in an ice bath, added to a prewarmed culture medium, and transferred to a 100 mm dish, which was then placed in an incubator at 37 °C for 1 h. Prior to confocal and STED imaging, the cells were washed three times with fresh DMEM to remove free, unbound BSA-conjugated FNDs, followed by reseeding and culturing on glass coverslips overnight. The specimens were finally fixed with 4 % paraformaldehyde on the coverslips, which were then sealed by using Mowiol as the embedding medium.[33]

For the biolabeling of HeLa cells with BSA-conjugated FNDs through endocytosis, the cells were first precultured on glass coverslips in 35 mm dishes at a density of approximately 2×10^5 cells per dish. The glass coverslips were then placed in a 35 mm dish seeded with BSA-conjugated FNDs (150 μg mL^{-1}) in PBS at 4 °C for 2 h. To avoid the otherwise inevitable precipitation of the particles on the specimens, the special precaution was taken to place the coverslips upside down on two fixed glass supports. The cells, after incubation and subsequent washing with PBS to remove unbound FNDs, were recultured in fresh culture medium at 37 °C for 3 h. They were then fixed with 4 % paraformaldehyde and sealed in Mowiol.[33]

The distribution of FNDs in cells was assayed by using a home-made stage-scanning confocal and STED microscope. The FNDs were excited with a CW Nd:YAG laser (DPSS 532, Coherent) focused onto the sample with a high-numerical-aperture oil-immersion microscope objective (HCX PL APO 100x, NA 1.4, Leica). Fluorescence was collected by the same objective, imaged onto a multimode fiber whose aperture worked as a confocal pinhole, and detected by an avalanche photodiode (APD) in single-photon counting mode. For STED imaging, a CW tunable Ti-sapphire laser (3900S, Newport) running at 740 nm depleted the FND fluorescence signal. A 0–2π vortex-generating phase mask (VPP-1, RPC Photonics) produced a helical phase retardation and a doughnut-shaped spot in the focal plane of the microscope objective, where the STED laser beam was overlapped with the excitation laser beam. The undepleted fluorescence was collected through a band-pass filter (FF01-685/40-25, Semrock) and a short-pass filter (ET700sp-2p, Chroma) and was detected with the same APD used for confocal imaging (see the Supporting Information for details). The images shown herein were typically acquired with an excitation laser power of 100 μW and a STED laser power of 180 mW.

Received: November 17, 2010
Published online: February 2, 2011

Keywords: endocytosis · fluorescence · nanodiamond · nanoparticles · STED microscopy

[1] *Applied Physics of Carbon Nanotubes: Fundamentals of Theory, Optics and Transport Devices* (Eds. S. V. Rotkin, S. Subramoney), Springer, New York, **2005**.
[2] G. Davies, M. F. Hamer, *Proc. R. Soc. London Ser. A* **1976**, *348*, 285 – 298.
[3] A. Gruber, A. Dräbenstedt, C. Tietz, L. Fleury, J. Wrachtrup, C. von Borczyskowski, *Science* **1997**, *276*, 2012 – 2014.
[4] S.-J. Yu, M.-W. Kang, H.-C. Chang, K.-M. Chen, Y.-C. Yu, *J. Am. Chem. Soc.* **2005**, *127*, 17604 – 17605.
[5] C.-C. Fu, H.-Y. Lee, K. Chen, T.-S. Lim, H.-Y. Wu, P.-K. Lin, P.-K. Wei, P.-H. Tsao, H.-C. Chang, W. Fann, *Proc. Natl. Acad. Sci. USA* **2007**, *104*, 727 – 732.
[6] J.-I. Chao, E. Perevedentseva, P.-H. Chung, K.-K. Liu, C.-Y. Cheng, C.-C. Chang, C.-L. Cheng, *Biophys. J.* **2007**, *93*, 2199 – 2208.
[7] F. Neugart, A. Zappe, F. Jelezko, C. Tietz, J. P. Boudou, A. Krueger, J. Wrachtrup, *Nano Lett.* **2007**, *7*, 3588 – 3591.
[8] O. Faklaris, D. Garrot, V. Joshi, F. Druon, J.-P. Boudou, T. Sauvage, P. Georges, P. A. Curmi, F. Treussart, *Small* **2008**, *4*, 2236 – 2239.
[9] M.-F. Weng, S.-Y. Chiang, N.-S. Wang, H. Niu, *Diamond Relat. Mater.* **2009**, *18*, 587 – 591.
[10] N. Mohan, C.-S. Chen, H.-H. Hsieh, Y.-C. Wu, H.-C. Chang, *Nano Lett.* **2010**, *10*, 3692 – 3699.
[11] V. Vaijayanthimala, H.-C. Chang, *Nanomedicine* **2009**, *4*, 47 – 55.
[12] Y. Xing, L. Dai, *Nanomedicine* **2009**, *4*, 207 – 218.
[13] S. W. Hell, *Nat. Methods* **2009**, *6*, 24 – 32.
[14] E. Rittweger, K. Y. Han, S. E. Irvine, C. Eggeling, S. W. Hell, *Nat. Photonics* **2009**, *3*, 144 – 147.
[15] K. Y. Han, K. I. Willig, E. Rittweger, F. Jelezko, C. Eggeling, S. W. Hell, *Nano Lett.* **2009**, *9*, 3323 – 3329.
[16] Y. Yuan, Y. Chen, J. H. Liu, H. Wang, Y. Liu, *Diamond Relat. Mater.* **2009**, *18*, 95 – 100.
[17] T. Takimoto, T. Chano, S. Shimizu, H. Okabe, M. Ito, M. Morita, T. Kimura, T. Inubushi, N. Komatsu, *Chem. Mater.* **2010**, *22*, 3462 – 3471.
[18] J. K. Lim, S. A. Majetich, R. D. Tilton, *Langmuir* **2009**, *25*, 13384 – 13393.
[19] K. Hanaki, A. Momo, T. Oku, A. Komoto, S. Maenosono, Y. Yamaguchi, K. Yamamoto, *Biochem. Biophys. Res. Commun.* **2003**, *302*, 496 – 501.
[20] S. H. Brewer, W. R. Glomm, M. C. Johnson, M. K. Knag, S. Franzen, *Langmuir* **2005**, *21*, 9303 – 9307.
[21] E. A. Permyakov, L. J. Berliner, *FEBS Lett.* **2000**, *473*, 269 – 274.
[22] T.-L. Wee, Y.-W. Mau, C.-Y. Fang, H.-L. Hsu, C.-C. Han, H.-C. Chang, *Diamond Relat. Mater.* **2009**, *18*, 567 – 573.
[23] T. Y. Tsong, *Biophys. J.* **1991**, *60*, 297 – 306.
[24] M. Marsh, H. T. McMahon, *Science* **1999**, *285*, 215 – 220.
[25] X. L. Kong, L. C. L. Huang, C.-M. Hsu, W.-H. Chen, C.-C. Han, H.-C. Chang, *Anal. Chem.* **2005**, *77*, 259 – 265.
[26] L.-C. L. Huang, H.-C. Chang, *Langmuir* **2004**, *20*, 5879 – 5884.
[27] B. Zhang, Y. Li, C.-Y. Fang, C.-C. Chang, C.-S. Chen, Y.-Y. Chen, H.-C. Chang, *Small* **2009**, *5*, 2716 – 2721.
[28] O. Faklaris, V. Joshi, T. Irinopoulou, P. Tauc, M. Sennour, H. Girard, C. Gesset, J.-C. Arnault, A. Thorel, J.-P. Boudou, P. A. Curmi, F. Treussart, *ACS Nano* **2009**, *3*, 3955 – 3962.
[29] Y.-R. Chang, H.-Y. Lee, K. Chen, C.-C. Chang, D.-S. Tsai, C.-C. Fu, T.-S. Lim, Y.-K. Tzeng, C.-Y. Fang, C.-C. Han, H.-C. Chang, W. Fann, *Nat. Nanotechnol.* **2008**, *3*, 284 – 288.
[30] K.-K. Liu, C.-C. Wang, C.-L. Cheng, J.-I. Chao, *Biomaterials* **2009**, *30*, 4249 – 4259.
[31] N. Mohan, Y.-K. Tzeng, L. Yang, Y.-Y. Chen, Y. Y. Hui, C.-Y. Fang, H.-C. Chang, *Adv. Mater.* **2010**, *22*, 843 – 847.
[32] See, for example, biotin-labeled bovine albumin from Sigma (catalogue no. A8549).
[33] C.-A. Wurm, D. Neumann, R. Schmidt, A. Egner, S. Jakobs in *Live Cell Imaging: Methods and Protocols* (Ed.: D.-B. Papkovsky, Humana Press, Totowa, NJ, **2010**, 185 – 199 (Methods in Molecular Biology 591).

